

Photospheric Signatures Of Solar Flares

Priya. Desai¹ · Richard Bogart¹ ·
Sebastian Couvidat¹ · Hugh Hudson² ·
Jesper Schou¹

© Springer ●●●●

Abstract We investigate flare related changes in the photospheric absorption line (Fe I 617.3 nm) profile in a large sample of solar flares of varying X-ray and H-alpha class, observed with the Helioseismic and Magnetic Imager (HMI) instrument aboard the Solar Dynamic Observatory (SDO). A distinct continuum enhancement, along with a corresponding decrease in line-depth is observed in over 40% of the flares. This continuum brightening can be observed in flares down to GOES X-ray class C 5.0. In most cases, the corresponding brightening in line-core is significantly larger than the observed continuum brightening, suggesting that the line formation is more sensitive to flare effects than the continuum. In powerful flares (example: GOES X6.9(SOL2011-08-09T08:05) and GOES X1.9 (SOL2011-09-24T09:40)) we observe the absorption line profile temporarily reverses direction and goes into emission during the flare. In this paper we present observations from three flares: SOL2011-09-24T09:40, an X1.9 flare where the absorption line briefly goes into emission; SOL2011-09-07T23:38, a X1.8 flare which shows noticeable reduction in line-depth and continuum brightening but does not go into emission; and SOL2010-11-04T23:58:00, a M1.6 flare which shows line-core brightening but no significant continuum enhancement.

Keywords: Solar Dynamics Observatory, continuum, absorption line, photosphere, white-light flares, HMI

1. Introduction and Motivation

A solar flare is an explosive release of energy stored in twisted magnetic fields, usually above or near sunspots. The term white-light Flare's (WLF's) has traditionally (Carrington, 1859) been used to designate solar flares observable as transient brightenings in the visible continuum. WLF's are important in flare research because they represent a large fraction of the radiated energy of a flare (eg. Neidig, 1989) and may challenge our current understanding of flare energy transport.

¹ Stanford University, Stanford, CA, USA;
email:priya@solar.stanford.edu

² Space Sciences Laboratory, University of California,
Berkeley, CA, USA

It is currently believed that the visible continuum is enhanced in all flares, but that the weaker ones are not detected as the signal is lost in the normal spatial and temporal fluctuations of the photosphere. Furthermore, even in strong flares, of small spatial extent ($\lesssim 5$ Mm), and of short duration ($\lesssim 250$ s), a systematic observation of the white-light component of flares has been historically challenging as it is difficult to serendipitously capture a flare at the right time and location for a spectroscopic observation, and most measurements (including space-based ones) do not have the temporal resolution to adequately observe the WL continuum near sunspots with low signal and contrast. In fact, prior to 1993 (Neidig *et al.* 1991), only ~ 86 WLF's had been reported and white-light emissions were only detected in flares above GOES magnitude X2. A study of white-light flares observed by Hinode (Wang, H, 2009) found the detectability threshold to be around M1 flares. Hudson, *et.al.* (2006) used white-light observations from the Transitional Region and Coronal Explorer (TRACE) with a spatial resolution of $1''$ and detected white-light emission for events as weak as GOES C2.0. Jess *et al* (2008) detected intense white-light emission in the blue continuum for a C1.6 flare using the diffraction-limited observations of the Swedish 1-meter Solar Telescope.

Motivated by this renewed interest in white-light flares, which we define as flares exhibiting enhanced emission in parts of the spectrum originating at or near the height of the the visible continuum photosphere, we set out to determine if we could detect photospheric flare signatures using the Helioseismic and Magnetic Imager (HMI) instrument on the Solar Dynamics Observatory (SDO), launched on February 11, 2010. The HMI instrument provides images in a photospheric line, Fe I 617.3 nm, at sufficient spatial and temporal resolution to resolve flare signatures and provide continuous images during the flare. Measurements of the line strength and nearby continuum brightness along with Doppler shift and Zeeman splitting and covering the whole solar disc, are available at a spatial scale of $0.5''$ once every 45 sec. Full-disc filtergrams in different polarizations and wavelengths across the line are available every 1.875 sec, offering the potential of high time resolution of the photospheric signatures of solar flares, provided that they can be detected and adequately measured. Thus, we have an opportunity to study the profiles of a large sample of flares of varying magnitudes using the same instrument, unlike previous ground based observations, which typically were with slit spectrographs providing fairly limited coverage (e.g. Neidig, 1989; Babin & Koval, 2007).

2. Observations and Data Reduction

Since a strong correlation is known to exist between X-ray emission and observed continuum brightening (Neidig, 1989), we chose to analyze a large sample of candidate flares belonging to GOES X-ray class X6.9 to class C1.5. In addition we also looked for flare-related photospheric effects in H-alpha flares that did not have an established detected X-ray counterpart. We primarily examined the HMI observables during the flares in order to establish the quantities most likely to be affected over the course of a flare, and their typical behavior. For this

Table 1. Characteristics of the flares chosen for this study.

Date	GOES Peak Time(UT)	AR Number	Location	Flare Class	Comments
2010.11.04	23:58	11121	S20 E76	M1.6	line-core brightening but no continuum brightening.
2011.09.07	22:38	11283	N14 W30	X1.8	line-core brightening and continuum brightening.
2011.09.24	09:40	11302	N13 E61	X1.9	line-core brightening, continuum brightening and line goes into emission.
2011.08.09	08:05	11263	N14 W69	X6.9	line-core brightening, continuum brightening and line goes into emission.

paper however, we have present observations from three representative flares that seem to best demonstrate the different observed photospheric effects: SOL2011-09-24T09:40, an X1.9 flare where the absorption line briefly goes into emission; SOL2011-09-07T23:38, a X1.8 flare which shows noticeable reduction in line-depth and continuum brightening but does not go into emission; and SOL2010-11-04T23:58:00, a M1.6 flare which shows line-core brightening but no significant continuum enhancement (See Table 1).

Five HMI observables, continuum intensity (I_c), line depth (L_d), line-width (L_w), dopplergrams (V), and magnetograms (M) are available every 45 sec. In order to produce these quantities however, HMI produces a nearly continuous stream of full-disc images of the sun in a set of six narrow wavelength bands (FWHM 76 mÅ) clustered around the central wavelength of an Fe I photospheric absorption line as 6173Å (See Schou *et al.* 2012). The filtergrams are made at a cadence of one every 1.875 second. They are taken in six combinations each of circular and linear polarization states in order to provide a full set of Stokes parameters for determination of the physical observables. The full sequence of all possible filtergrams repeats at a period of 135 s; the repetition period of filtergrams necessary to produce the intensity and Doppler observables is one-third that, so they are available at a cadence of 45s, the basic cadence Image stabilization provides spatial stability of 0.03 arc-sec throughout the complete sequences of filtergrams required for the observables. The per-pixel statistical noise for filtergrams is approximately 0.3%. Exposure time knowledge is considerably better, about 0.002%, and for the continuum intensity measurement, combining all filtergrams over a 45-sec frame sequence, the per-pixel noise is about 0.1%.

We use tracked, 45s cadence, continuum (I_c) and and line-depth (L_d) data for a period one hour or ninety minutes (30/45 minutes before and after the

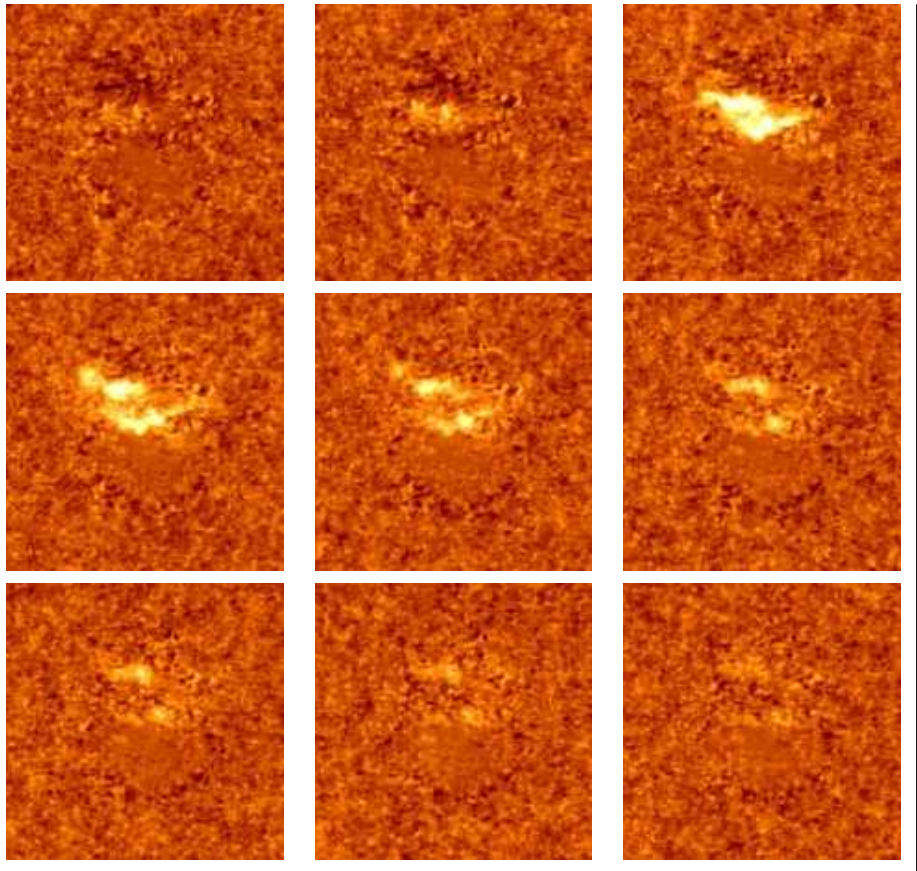


Figure 1. Brightening observed in the line-core images for SOL2011-09-07T22:38:00 for selected times before and during the flare. The region shown is a $6^\circ \times 6^\circ$ square, suitably tracked and mapped to a grid centered at latitude $15^\circ.64$ N and Carrington longitude $226^\circ.09$, the nominal location of the flare. Each image is 90s apart.

flare) to determine the “line-core” profile behavior during the flare. We define the “line-core” value at a pixel as the difference between the continuum intensity and the line-depth values at that pixel. Instead of using the standard observables, we used observables calculated using the algorithm normally reserved for the Near-Real Time (NRT) data, since the standard HMI observables are produced using a weighting function extending over 135 seconds before and after the “recorded-time” and has negative side lobes in the range ± 45 -90 seconds. While providing more accurate results under normal circumstances, the standard interpolation scheme may result in spurious artifacts in the case of transient events (see Martinez-Oliveros *et.al.* 2011). The NRT algorithm, on the other hand, involves simple 2-point (linear) interpolation with positive-definite weightings among filtergrams within 45 seconds of the represented time. We deem the observed and so-produced data to be more an accurate representation

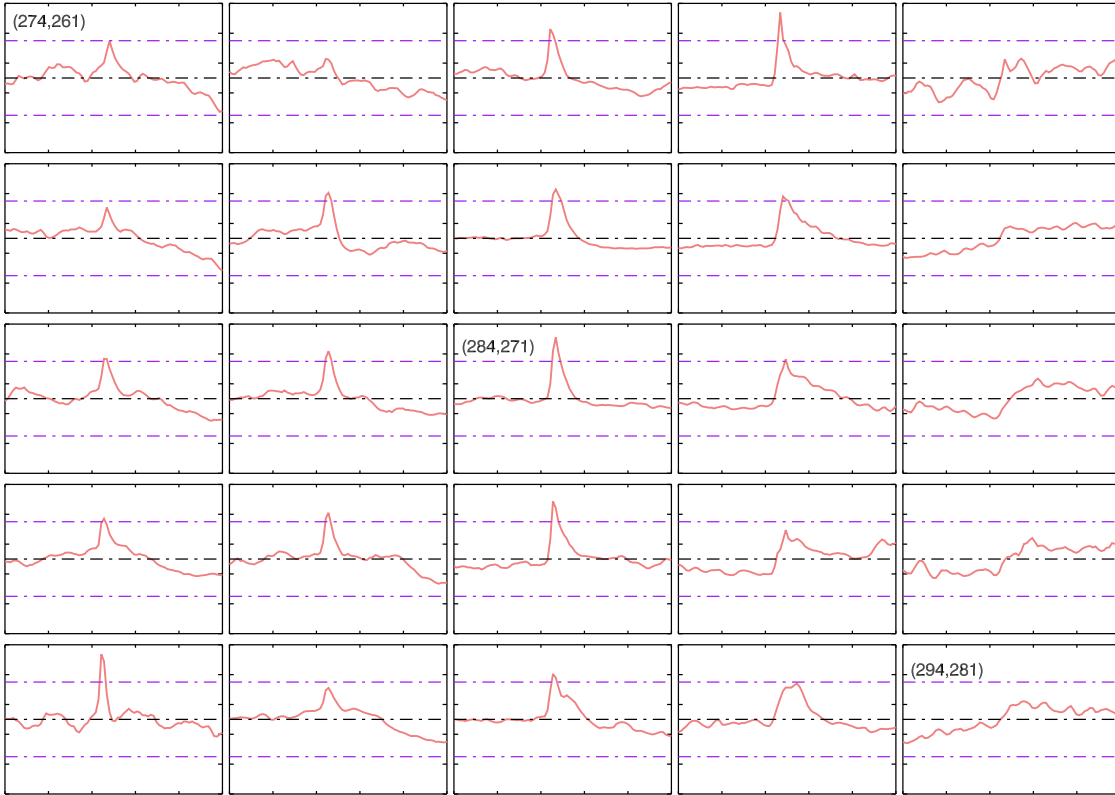


Figure 2. Mosaic of the time variation plots of the line-core intensity ($I_c - L_d$ using NRT values) for a section of the active region that produced the flare SOL2011-09-07T22:38:00. Each plot corresponds to a single pixel, and light-curves are plotted for every fifth pixel in a region covering a 20×20 pixels. The central pixel labeled (284,271) is located at $15^\circ.53$ N and $30^\circ.6$ W (Carrington longitude $226^\circ.5$). The horizontal (time) axis spans 60 minutes. The vertical axis spans minimum and maximum of the line-core intensity in that period. The central dotted line is the mean line-core value for that pixel over the 60 minutes duration, and top and bottom dotted horizontal lines correspond to $\pm 6 \sigma$ from the mean line-core value.

of the line profile during an impulsive phenomenon. In the following analysis, we only use the NRT algorithm data as well as the individual HMI filtergrams which have also been interpolated in time (using the same target time).

3. Discussion and Results

The images and plots in Figures 1-4 are from flare SOL2011-09-07T22:38:00, of GOES class X1.8. Figure 1 is a typical time sequence of tracked and mapped images of the line-core during the flare. The images are taken 90 seconds apart. Fig 2 illustrates the temporal variation in the line-core over a period of one hour (including during the flare) of twenty-five pixels chosen from a grid of 20×20 pixels. Each plot corresponds to a single pixel, and light-curves are plotted for every fifth pixel in the region covering the 20×20 pixels. The central pixel

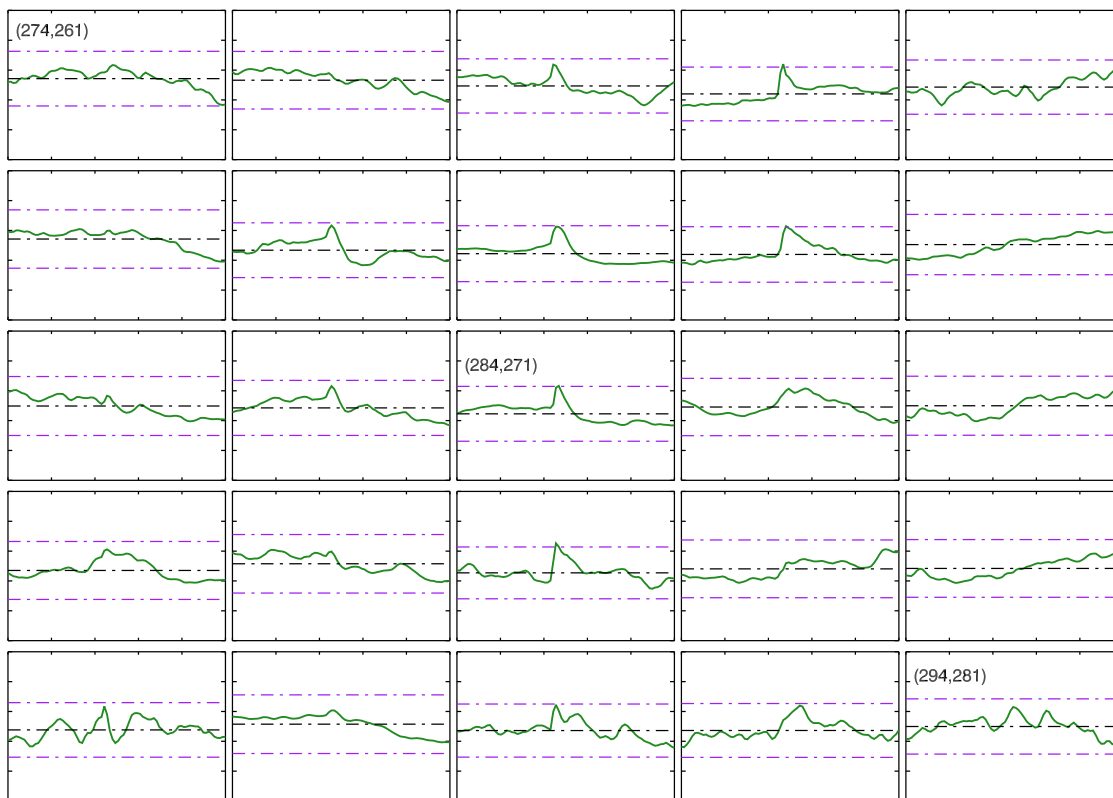


Figure 3. Mosaic of the time variation plots of the continuum intensity (NRT I_c) for the same section of the active region of flare SOL2011-09-07T22:38:00 as shown in Figure 2. Again, the horizontal axis spans 60 minutes but the vertical axis range includes the minimum and maximum continuum intensity values within that time period. The central dotted line is the mean (NRT) continuum value for that pixel over the 60 minutes duration, and top and bottom dotted horizontal lines correspond to $\pm 6\sigma$ from the mean continuum value.

labeled (284, 271) is located at $15^\circ.53$ N and $30^\circ.6$ W. The horizontal axis spans 60 minutes. The central dotted line is the mean line-core value for that pixel over the 60 minutes duration, and top and bottom dotted horizontal lines correspond to $\pm 6\sigma$ from the mean line-core value. Note that these plots are made using tracked “NRT” data. As can be seen, a large number of the pixels show greater than a 6σ increase in the line core suggesting a strong enhancement.

Figure 3 shows a mosaic of plots of continuum intensity vs time for all the same pixels as Figure 2. However, fewer number of pixels show a 6σ increase in the continuum brightening as compared to the line core. Figure 4 is a plot of the six spectral intensities observed across the line profile before and during the flare at the central pixel (labeled 284, 271) of the mosaic in Figure 2 and 3. The line profile shows a significant continuum enhancement and line core enhancement. Examination of all the pixels where the line core brightening was observed indicates that the line strength never exceeds the continuum and the line always stays in absorption.

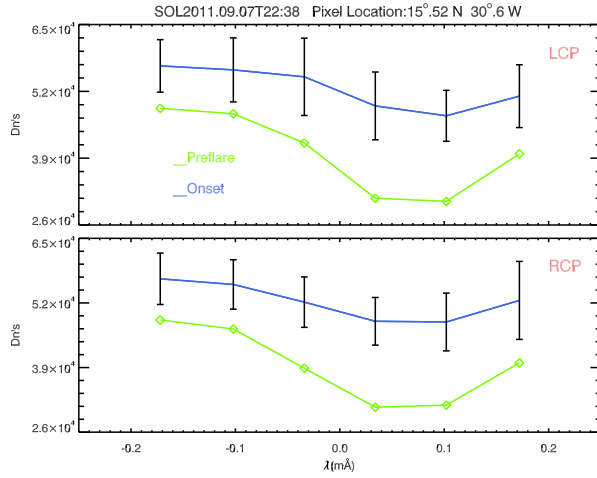


Figure 4. Spectral intensity across the HMI line for selected times before and during the flare for the central pixel (284 x 271) (i.e. at $15^{\circ}.53$ N and $30^{\circ}.6$ W) of the above mosaic in Figure 2 and 3. Intensities in both left-circularly-polarized (LCP) and right-circularly polarized (RCP) light are shown.

Figures 5-7 are from flare SOL2011-09-24T22:38:00 and include the line-core, continuum intensity and line-depth images of a $9^{\circ} \times 8^{\circ}$ region centered at $12^{\circ}.82$ N and $66^{\circ}.4$ E. Figure 8 shows a plot of the six spectral intensities (filtergrams) before and during the flare at two consecutive pixels located at latitude $12^{\circ}.56$ N (left) and $60^{\circ}.38$ E and $12^{\circ}.56$ N $60^{\circ}.42$ E (right). Temporal plots of the filtergrams show that at some pixels, that absorption line profile gets shallower as the flare progresses, and line core temporarily exceeds the continuum i.e the line goes into emission. Figure 8 shows the “pre-flare” and “flare onset” profiles of two such pixels where the line profile is in absorption before the onset of the flare and then goes into emission during the flare. Plots of the six-point spectra along with the known Doppler velocity in the region of the flare were used to determine the “true continuum”. Past observations of flares (Babin & Koval, 2007, Lozitsky, 2007) suggest that while central emission features have been observed in the line-core before, observations of the entire line going into emission may be rare. However, we have observed similar line emission profiles in the flare SOL2011-08-09T08:05:00 (X6.9) suggesting they may be more common than believed in the past.

Figures 9-12 refer to the flare SOL2010-11-04T23:58:00, GOES M1.6. Figures 9-11 are a mosaic of the temporal variations in line-core, continuum and equivalent width in a period of one hour including the duration of the flare, from twenty-five pixels chosen from a grid of 20×20 pixels centered at. As can be seen, from Figures 9 and 10, the line-core enhancement is significantly more pronounced than the continuum. The equivalent depth is calculated as: $E_w = L_d * L_w / I_c * \text{constant}$.

Temporal variations in the equivalent depth are plotted in Figure 11. (Note, we did not plot equivalent depths for the pixels for flares SOL2011-09-07T22:38 and SOL2011-09-24T22:38:00 as the line-width (L_w) and line-depth (L_d) could

not be accurately calculated for some of the the pixels). Examination of the filtergrams for flare SOL2010-11-04T23:58:00 reveals that the line stays in absorption over the entire duration of the flare. Figure 12 is a typical plot of the the filtergram spectral intensities and show no significant increase in the continuum.

Analysis of all X class flares observed by HMI (nine so far), reveals that an increase in the continuum is observed is in all the flares, suggesting that all the X-class flares could be categorized at white-light flares. The combination of an overall increase in brightness, the lower base level of line-core intensity, and the reduced absorption in the line implies that the line-core intensity is a more sensitive indicator of the flare than continuum intensity.

In the case of the M-class flares, a similar line-core enhancement was observed in approximately 45 out of the 100 flares investigated, but only 21 of those 45 showed a detectable increase in the continuum. Figure 3 shows the normalized line-core, continuum and equivalent width of a flaring pixel from the M 9.0 flare on July 30th, 2011. There is a strong temporal correlation between the X-ray flux and photospheric effects. The line-core intensity enhancement is again more pronounced than the continuum enhancement.

X-class flares reveal that an increase in the continuum is observed is in all the flares, suggesting that all the X-class flares could be categorized at white-light flares. The combination of an overall increase in brightness, the lower base level of line-core intensity, and the reduced absorption in the line means that the line-core intensity may be a more sensitive indicator of the flare than continuum intensity.

In the case of other M-class flares, a similar line-core enhancement is observed in approximately 45 out of the 100 flares investigated, but only 21 of those 45 showed a detectable increase in the continuum. All the flares show a strong temporal correlation between the X-ray flux and photospheric effects. However, the line-core intensity enhancement is again more pronounced than the continuum enhancement.

Similar brightenings in the line-core are detected in flares with GOES class greater than C 5.0 and possibly in a few of the H alpha flares. In many cases, continuum enhancement was not detectable in all the cases where a line-core increase was measurable, but for all cases with continuum enhancement, the line-core strengthening (and line-depth reduction) was equivalent or significantly larger, suggesting that in general, the line-core enhancement is a far more robust marker for photospheric effects than the continuum brightening associated with genuine white-light flares. The 45s cadence "NRT" HMI observables along with the individual filtergrams provide sufficient spatial and temporal resolution to observe the evolution of the flare.

4. Summary

We have detected a photospheric continuum brightening in a large number of flares. Many of these would traditionally have classified as WLF's. However, the relative enhancement in the line-core profile is significantly stronger than that observed in the continuum and is sometimes detectable even when there is no significant continuum enhancement. The line-core intensity sometimes temporarily

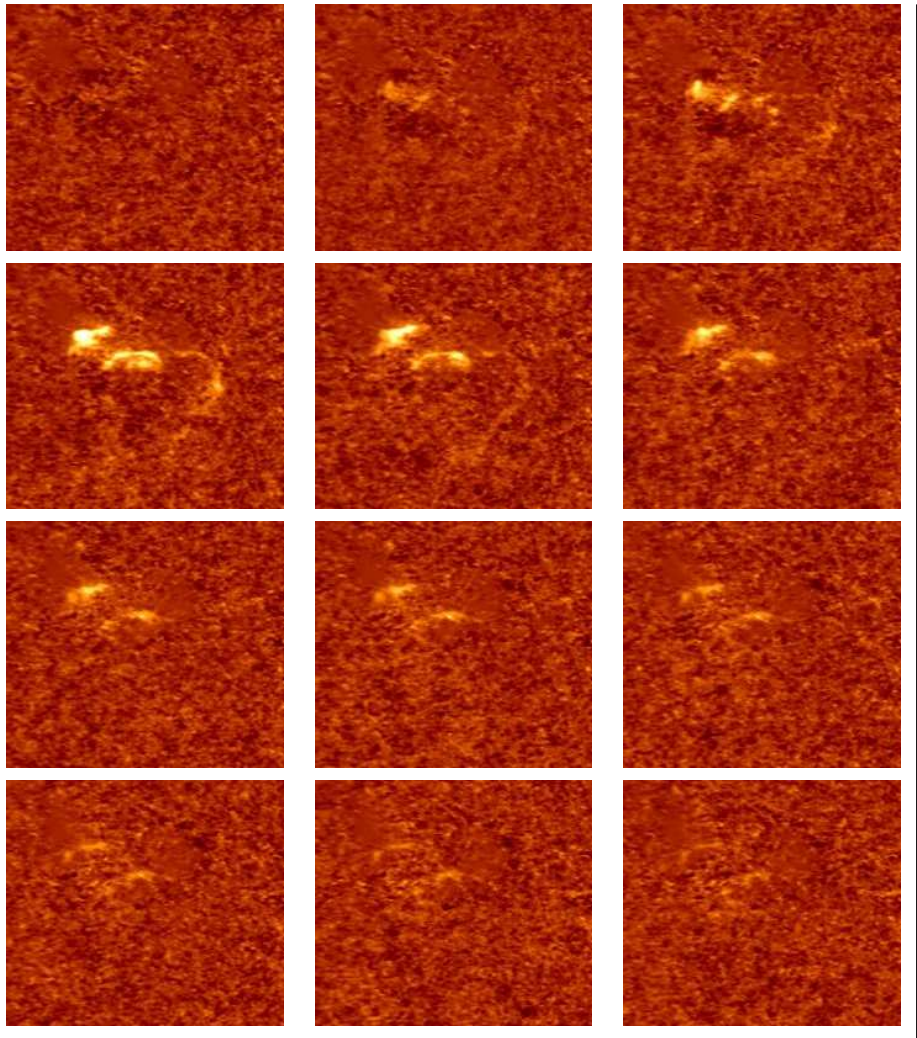


Figure 5. Brightening observed in the line-core images for SOL2011-09-24T22:38:00 for selected times before and during the flare. The region shown is a $9^\circ \times 8^\circ$ rectangle, suitably tracked and mapped to a grid centered at latitude $12^\circ.82$ N $66^\circ.4$ E. Each image is taken 1 min 15sec apart.

exceeds the continuum emission, thus temporarily reversing the absorption line into an emission line. The observed emission may last for over a minute before the line profile returns to absorption.

The line-core intensity calculated with the NRT algorithm are more useful than the standard 45s-HMI observables. The flares so observed are spatially and temporally well correlated to the GOES X-ray events, indicating that HMI can be used to systematically study and track the photospheric effect of flares.

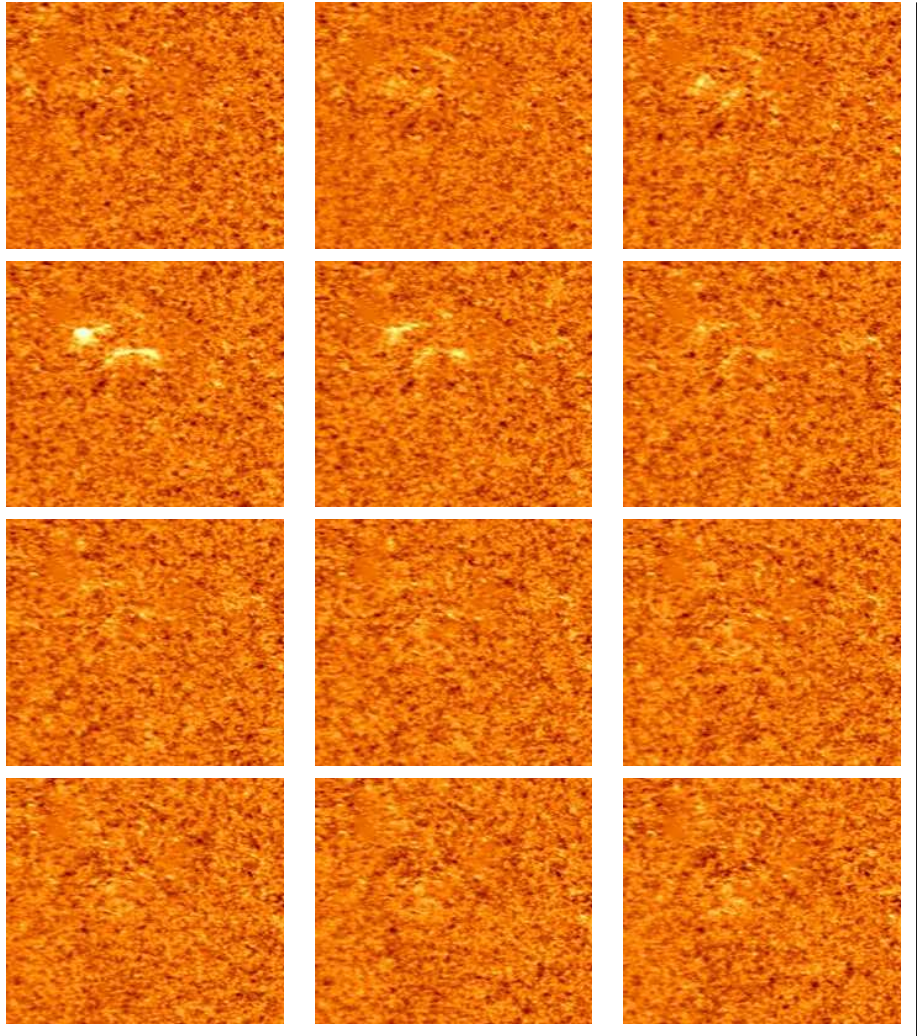


Figure 6. Brightening observed in the continuum (I_c observable for SOL2011-09-24T22:38:00 for selected times before and during the flare. The region shown is a $9^\circ \times 8^\circ$ rectangle, suitably tracked and mapped to a grid centered at latitude $12^\circ.82$ N $66^\circ.4$ E. Each image is taken 1 min 15sec apart

References

- Abramenko, V.I., and Baranovsky, E.A., 2004, *Solar Phy.*, **220**, 81-91.
 Babin, A.N., and Koval, A.N., 2007, *Bulletin of the Crimean Astrophysical Observatory*, **103**, 63
 Babin, A.N., and Koval, A.N., 2008, *Bulletin of the Crimean Astrophysical Observatory*, **104**, 11
 Carrington, R.C. *M.N.R.A.S.*, **20**, 13.
 Hudson, H. S., Wolfson, C. J., & Metcalf, T. R., 2006 *Solar Phys.*, **234**, 79

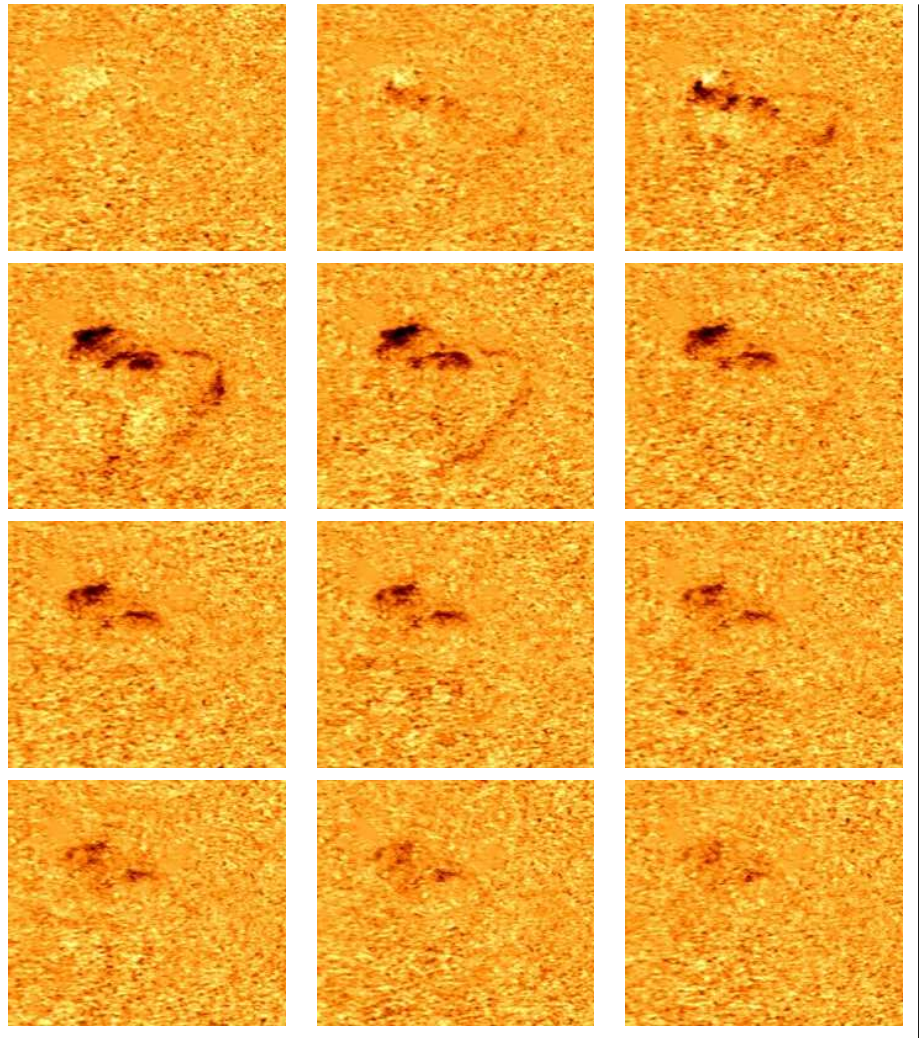


Figure 7. Brightening observed in the line-depth (L_d) observable for SOL2011-09-24T22:38:00 for selected times before and during the flare. The region shown is a $9^\circ \times 8^\circ$ rectangle, suitably tracked and mapped to a grid centered at latitude $12^\circ.82$ N $66^\circ.4$ E. Each image is taken 1 min 15sec apart

- Jess, D. B., Mathiaoudakis, M., Crockett, P.J., and Keenan, F.P., 2008, *Astrophys. J.Lett*, **688**, 119.
- Lozitsky, V.G., 2009, *Astronomy .Lett*, **35**, 136.
- Neidig, D. F., Wilborg, P. H., & Gilliam, L. B., 1993 *Solar Phys.*, **144**, 169.
- Martinez-Oliveros, J.C., Couvidat, S., Schou, J., Krucker, S., Linsey, C., Hudson, H.S., & Scherrer, P., 2011, *Solar Phy.*, **269**, 269.
- Wang, H. M., 2009. *Research in Astronomy and Astrophysics.*, **9**, 127.
- Schou, J. et al., 2004, *Helioseismic and Magnetic Imager for Solar Dynamics Observatory: Instrument Performance Document*, <http://hmi.stanford.edu/>

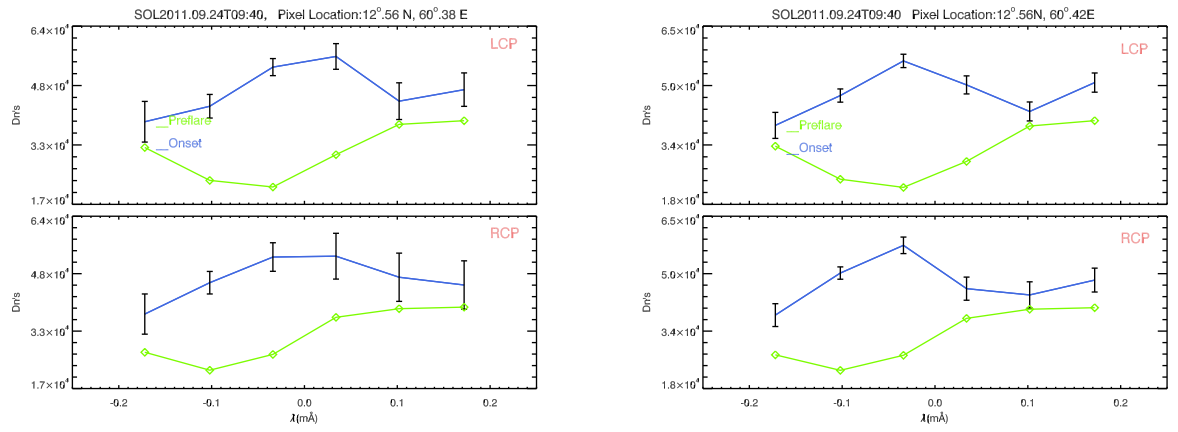


Figure 8. The six point spectral intensities (in LCP and RCP) of the pixels located at latitude 12° 56 N (left) and 60° 38 E and 12° 56 N 60° 42 E (right) before and during the flare SOL2011-09-24T22:38:00. These “profiles” show that the line strength changes to a greater extent than the continuum during the flare, and the line goes briefly into emission.

Schou, J., Cherrier, P. H., Bush, R. I., Wachter, R., & Couvidat, S. *et al.*, 2012, *Solar Phys.*, **275**, 229. (DOI: 10.1007/s11207-011-9709-6)

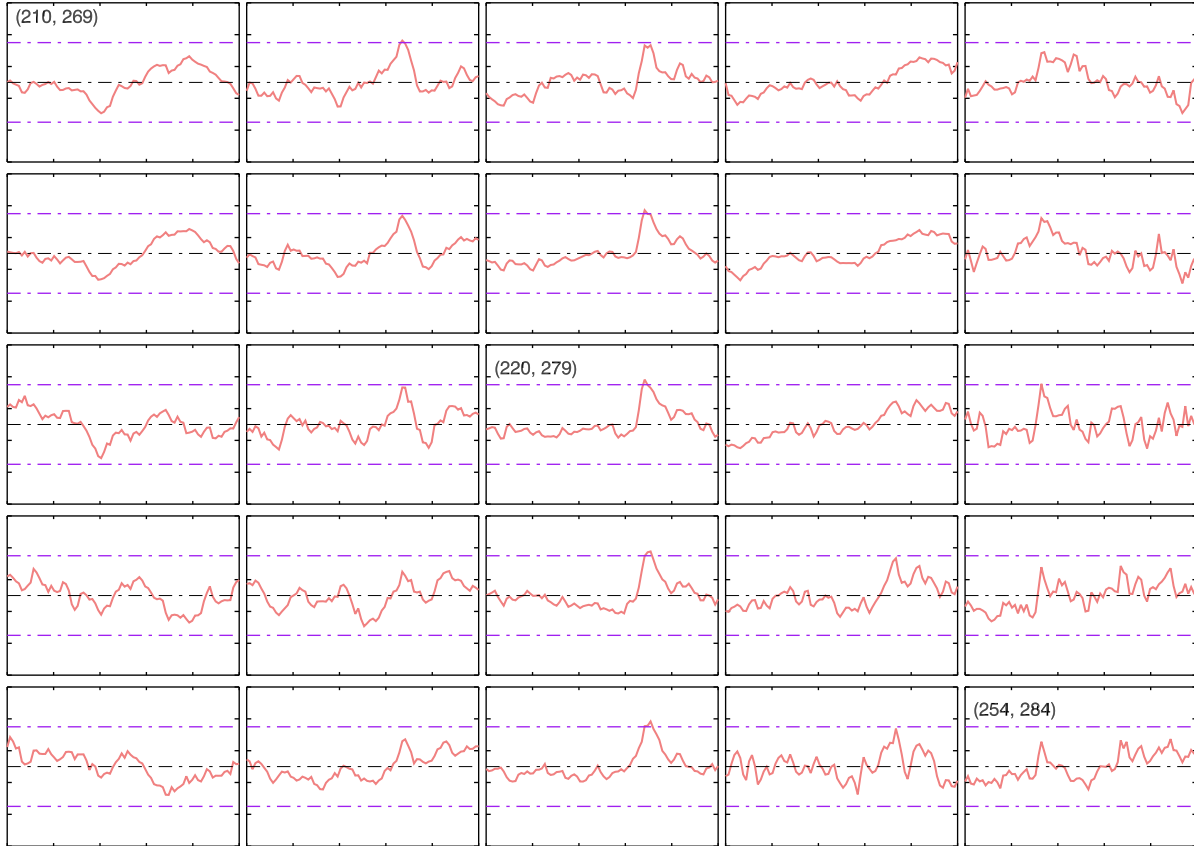


Figure 9. Mosaic of the time variation plots of the line-core intensity ($I_c - L_d$ using NRT values) for a section of the active region that produced the flare SOL2010-11-04T23:58:00. Each plot corresponds to a single pixel, and light-curves are plotted for every fifth pixel in a region covering a 20×20 pixels. The central pixel labeled (220,279) is located at $18^\circ.56$ S and $75^\circ.08$ E. The horizontal(time) axis spans 60 minutes. The vertical axis spans minimum and maximum of the line-core intensity in that period. The central dotted line is the mean line-core value for that pixel over the 60 minutes duration, and top and bottom dotted horizontal lines correspond to $\pm 6 \sigma$ from the mean line-core value.

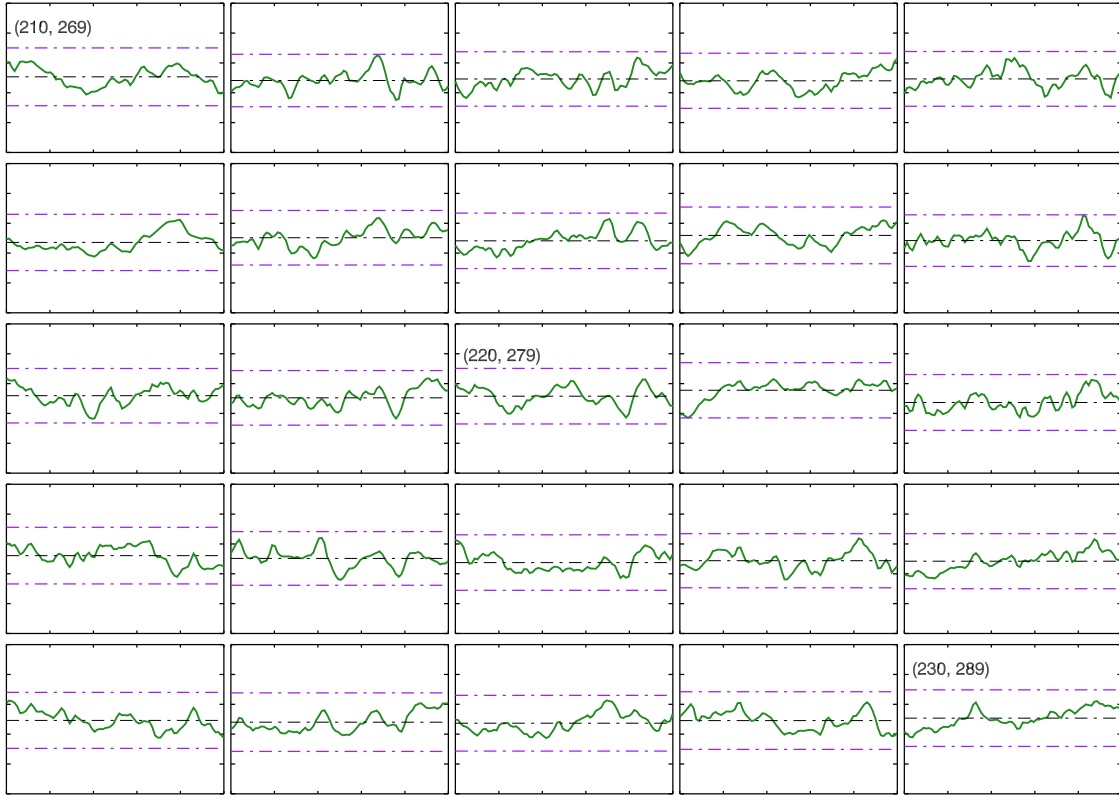


Figure 10. Mosaic of the time variation plots of the continuum intensity (I_c using NRT values) for a section of the active region that produced the flare SOL2010-11-04T23:58:00. Each plot corresponds to a single pixel, and light-curves are plotted for every fifth pixel in a region covering a 20×20 pixels. The central pixel labeled (220,279) is located at $18^\circ.56$ S and $75^\circ.08$ E. The horizontal (time) axis spans 60 minutes. The vertical axis spans minimum and maximum of the continuum intensity in that period. The central dotted line is the mean continuum value for that pixel over the 60 minutes duration, and top and bottom dotted horizontal lines correspond to $\pm 6 \sigma$ from the mean line-core value

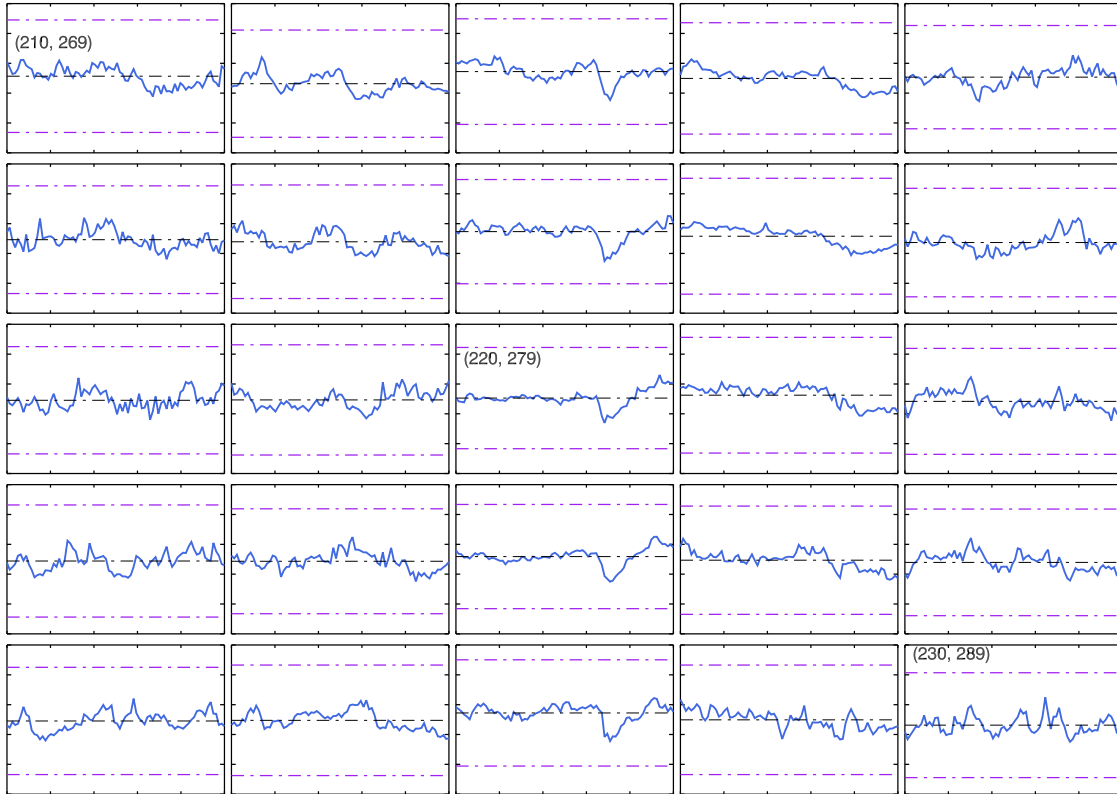


Figure 11. Mosaic of the time variation plots of the equivalent depth (E_w using NRT L_c , L_d and L_c values) for a section of the active region that produced the flare SOL2010-11-04T23:58:00. Each plot corresponds to a single pixel, and light-curves are plotted for every fifth pixel in a region covering a 20×20 pixels. The central pixel labeled (220,279) is located at $18^\circ.56$ N and $75^\circ.08$ E. The horizontal(time) axis spans 60 minutes. The vertical axis spans minimum and maximum of the equivalent depth values in that period. The central dotted line is the mean equivalent depth value for that pixel over the 60 minutes duration, and top and bottom dotted horizontal lines correspond to $\pm 6 \sigma$ from the mean equivalent-depth value.

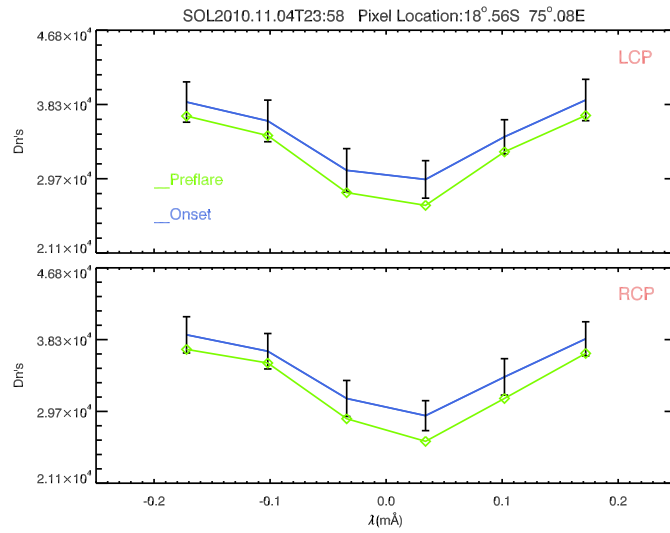


Figure 12. The six point spectrum before, during and after the flare SOL2010-11-04T23:58 (M1.6) over time showing a very small increase in the continuum intensity.